Received: 24 April 2021 | Revised: 18 June 2021 | Accepted: 28 June 2021

DOI: 10.1002/jemt.23867

RESEARCH ARTICLE

MICROSCOPY RESEARCH & TECHNIQUE WILEY

Precursor effects on the physical, biological, and catalytic properties of *Fagonia indica* Burm.f. mediated zinc oxide nanoparticles

Safia Hameed[1] | Ali Talha Khalil[2,3,4] | Muhammad Ali[1] | Javed Iqbal[5,6] | Lubna Rahman[1] | Muhammad Numan[1] | Saleh Khamlich[3,4] | Malik Maaza[3,4] | Ikram Ullah[7] | Banzeer Ahsan Abbasi[6] | Fawaz Alasmari[8] | Zabta Khan Shinwari[6]

[1]Department of Biotechnology, Quaid-i-Azam University, Islamabad, Pakistan

[2]Department of Pathology, Lady Reading Hospital, MTI, Peshawar, Pakistan

[3]UNESCO-UNISA Africa Chair in Nanosciences-Nanotechnology, College of Graduate Studies, University of South Africa, Pretoria, South Africa

[4]Nanosciences African Network (NANOAFNET), iThemba LABS-National Research Foundation, Somerset West, Western Cape, South Africa

[5]Department of Botany, Bacha Khan University, Charsadda, Khyber Pakhtunkhwa, Pakistan

[6]Department of Plant Sciences, Quaid-i-Azam University, Islamabad, Pakistan

[7]Biotechnology and Genetic Engineering, Hazara University, Mansehra, Pakistan

[8]Department of Pharmacology and Toxicology, College of Pharmacy, King Saud University, Riyadh, Saudi Arabia

Correspondence
Safia Hameed, Department of Biotechnology, Quaid-i-Azam University, Islamabad 46000, Pakistan.
Email: safiahameed77@gmail.com

Javed Iqbal, Center for Plant Sciences and Biodiversity, University of Swat, Kanju 19201, Pakistan.
Email: javed89qau@gmail.com

Review Editor: Mingying Yang

Abstract

We report a facile, green and precursor-based comparative study on the biosynthesis of zinc oxide (ZnO) nanoparticles (NPs) using anticancerous *Fagonia indica* as effective chelating agent. Biosynthesis was carried out using zinc sulfate and zinc acetate as precursor salts to make ZnO_S and ZnO_A NPs under similar experimental conditions which were characterized extensively for physical and biological properties. Scherrer equation deduced a mean crystallite size of ~23.4 nm for ZnO_A NPs and ~41 nm for ZnO_S NPs. The nature of the NPs was compared using UV, diffuse reflectance spectra, Fourier transform infrared spectroscopy, thermogravimetric analysis–DTA, selected area electron diffraction, EDS, zeta potential, high resolution (HR)-SEM, and HR-TEM. Detailed in vitro pharmacognostic activities revealed a significant therapeutic potential for ZnO_A and ZnO_S. Potential antimicrobial activities for the NPs and their nanocosmeceutical formulations are reported. ZnO_A NPs were more cytotoxic to *Leishmania tropica* as compared to ZnO_S. Significant antioxidant and protein kinase inhibition was obtained. The hemolytic assay indicated a hemocompatible nature of both ZnO_A and ZnO_S NPs. Catalytic degradation of crystal violet dye (CVD) by NPs was examined under different parameters (light, dark, UV). Furthermore, sonophotocatalytic degradation of CVD was also studied. Our results suggested that precursor can have a significant effect on the physical, biological, and catalytic properties of the NPs. In future, we recommend different other in vitro, in vivo biological activities, and mechanistic studies of these as-synthesized NPs.

KEYWORDS
antimicrobial, antioxidant, cytotoxic, *Fagonia indica*, ZnO nanoparticles

1 | INTRODUCTION

Modern day technologies like nanotechnology is at the forefront of research because of their multiple applications in environment, chemistry, energy, agriculture, medicine, communication technologies, and so forth. Materials at nanoscale are different from their macroscale counterparts as they possess distinctive electrical, chemical, optical physical, and thermal properties (Abbasi, Iqbal, Khan, et al., 2020; Haghniaz et al., 2021; Uddin, Safdar, Anwar, et al., 2021; Uddin, Safdar, Iqbal, et al., 2021). Recently, metal or metal-based nanoparticles (NPs) have gained tremendous importance because of their different applications (Abbasi, Iqbal, Nasir, et al., 2020; Shah

et al., 2021; Ullah et al., 2020). Among metal oxide NPs, zinc oxide NPs (ZnO NPs) are readily studied due to their multifunctional and tunable nature. The multifunctionality of ZnO NPs is evidenced from their uses in broad range applications like cosmetics, biomedicine, energy storage etc. ZnO NPs are represented by 3.37 eV direct band gap and high excitation energy (60 meV), making it an ideal material to be used in UV photodetectors, transistor, semiconductor diodes, and so forth (Iqbal, Abbasi, Ahmad, Mahmoodi, et al., 2020; Thema, Manikandan, Dhlamini, & Maaza, 2015). Furthermore, ZnO NPs are routinely used in mineral-based sunscreens, lotions, and ointments, while their potential for bioimaging and drug delivery has also been demonstrated (Hameed et al., 2019; Iqbal, Abbasi, Batool, et al., 2019). ZnO NPs can be synthesized using different physical and chemical methods. The chemical processes include pyrolysis (Saravanakkumar et al., 2018), sol–gel (Barhoum et al., 2017; Hameed et al., 2020), and sonochemical (Yadav, Mishra, & Pandey, 2008), while the physical methods include laser ablation (Gondal, Drmosh, Yamani, & Saleh, 2009), pulse laser deposition (Kawakami, Hartanto, Nakata, & Okada, 2003), chemical vapor deposition (Liu, Wu, Cao, & Chang, 2004), molecular beam epitaxy (Zhang et al., 2005), and so forth. Despite of being effective, these physical and chemical means are accompanied by considerable disadvantages like elevated energy consumption, cost, and toxicity (Iqbal, Abbasi, Ahmad, et al., 2019; Iqbal, Abbasi, Ahmad, Shahbaz, et al., 2020, Fuku et al., 2018). Toxic waste lines are generated as a result of chemical processes. Due to environmental issues and energy imbalance, greener methods for the synthesis of NPs are proposed which includes the use of therapeutic and natural extracts of the plant as a potential reducing, stabilizing, and capping agents (Khalil et al., 2017a; Khalil et al., 2017b; Ovais et al., 2017). As a result, a paradigm shift has been observed toward the application of biological resources for the synthesis of metal NPs (Kibasomba et al., 2018; Iqbal, Abbasi, Ahmad, Mahmoodi, et al., 2020; Iqbal, Abbasi, Ahmad, Shahbaz, et al., 2020; Iqbal, Abbasi, Munir, Uddin, et al., 2020; Mohamed et al., 2019). Other biological resources like bacteria and fungi may also be used; however, they raise biosafety concerns (Abbasi, Iqbal, Zahra, et al., 2020; Iqbal, Abbasi, Mahmood, Hameed, et al., 2019; Iqbal, Abbasi, Mahmood, Kanwal, et al., 2019). In addition, synthesis using microorganisms is challenging as it involve extensive and multiple steps for maintaining cell culture. Therefore, the medicinal plants are preferred over microbial means for synthesis of NPs. Medicinal plants generally has a rich phytochemistry and possess bioactive chemical entities like glycosides, flavonoid, terpenoids, alkaloids, saponins, inositol, resins, terpenes, volatile oils, tannins, and so forth (Abbasi et al., 2018; Abbasi, Iqbal, Mahmood, Qyyum, & Kanwal, 2019; Batool et al., 2020; Iqbal et al., 2017; Zahra, Iqbal, Abbasi, Shahbaz, et al., 2021; Zahra, Iqbal, Abbasi, Yaseen, et al.,) which can reduce and stabilize the NPs. Therefore, the interface of the nanosciences and medicinal plants is becoming increasingly popular for synthesizing metal NPs (Abbasi et al., 2019; Abbasi, Iqbal, Kiran, et al., 2020; Khalil et al., 2021; Uddin, Safdar, et al., 2021; Uddin, Safdar, et al., 2021).

Fagonia indica Burm.f. belongs to Zygophyllaceae is a popular medicinal plant is known for their potential anticancer activities. Locally *F. indica* is known as "Azghaki"/Pashto and "Dhamasa"/Urdu. Traditionally *F. indica* is many uses. It is used as blood purifier, febrifuge and also used for the treatment of small pox. Locally, it is also used for fever, asthma, dysentery, urinary discharge, liver and skin diseases, and so forth (Anil, Nikhil, Manoj, & Prakash, 2012). *F. indica* is also used traditionally in the treatment of diabetes (Ahmad, Qureshi, Arshad, Khan, & Zafar, 2009). Numerous biological activities of *F. indica* have been documented like anticancer, antimicrobial, antiseptic, antidiabetic, antioxidant, and anti-inflammatory (Rahman, Shinwari, Iqrar, Rahman, & Tanveer, 2017; Waheed et al., 2012).

Given the therapeutic potential, phytochemistry and excellent reported biological activities of *F. indica*, compelled us to investigate them from the perspective of green synthesis of ZnO NPs. Silver NPs have already been synthesized using *F. indica* (Ullah, Shinwari, & Khalil, 2017); however, to date, no work has been done on ZnO NPs. Different medicinal plants like *Azadirachta indica* (Bhuyan, Mishra, Khanuja, Prasad, & Varma, 2015), *Plectranthus amboinicus* (Fu & Fu, 2015), *Moringa oleifera* (Matinise, Fuku, Kaviyarasu, Mayedwa, & Maaza, 2017), and so forth have been ZnO NPs biosynthesis. In order to fulfill the vacuum in scientific literature, herein, we report a detailed and comparative study on the biosynthesis of ZnO NPs using the aqueous extracts of *F. indica*. ZnO NPs were synthesized using two different precursors, that is, zinc acetate and zinc sulfate. The study is of the first of its kind in which a precursor-based comparison was performed in terms of the physical and biological properties of ZnO NPs synthesized using the aqueous extracts of *F. indica*.

2 | EXPERIMENTAL

2.1 | Collection and processing of *F. indica*

The test material was collected from Peshawar, Khyber Pakhtunkhwa, Pakistan, and taxonomically verified as *F. indica* in the Herbarium of Islamabad (ISL), Quaid-i-Azam University; Islamabad. Fresh plant material was rinsed using distilled water to remove the dust and other particulate material, excised with sterile scissor and used for extraction. Extraction of the plant material was carried out as described previously with minor modifications (Khalil et al., 2017a; Khalil et al., 2017b). Briefly, the plant material (30 g of the excised aerial parts of the plant) was introduced to distilled water (250 ml) on a hotplate with magnetic stirrer for 3 hr at 80°C. The resultant brownish dye was filtered thrice to remove the waste material from liquid extracts by a Whatman filter and was allowed to cool at room temperature. The pH of the extract was determined as 6.34 at room temperature. The visually clear extracts were used further.

2.2 | Biosynthesis of ZnO NPs

Previously established method was applied to synthesize ZnO NPs (Thema et al., 2015). The biosynthesis reaction was carried out in a 250 ml reagent bottle. Briefly, 6 g of the precursor salts zinc acetate

dihydrate and zinc sulfate were added to the 100 ml of the obtained aqueous extracts separately. After the addition of zinc acetate and zinc sulfate, the pH was determined as 5.73 and 5.34, respectively. The reaction mixture was further heated on hotplate at 60°C for 2 hr with magnetic stirring. Later, the reaction mixture was allowed to cool at room temperature followed by centrifugation at 10,000 rpm for 10 min to obtain the precipitate which was subsequently washed three times with distilled water (10,000 rpm/10 min), dried (~3 hr at 100°C), followed by annealing at 500°C in a muffle furnace. The obtained grayish material (assumed as ZnO NPs) was further used for physical characterizations. The material obtained from zinc acetate dihydrate and zinc sulfate as precursors were labeled as ZnO_A and ZnO_S, respectively.

2.3 | Characterization of NPs

XRD pattern of the thermally annealed material was carried out using XRD diffractometer (Bruker) equipped with Kα of copper ($\lambda = 1.5406$ Å) irradiation line and Scherrer formula was used to determine the grain size (Equation (1)).

$$\text{Particle size} = {}^{K\lambda}/_{\beta\cos\theta} \quad (1)$$

Different spectroscopic techniques were used to elaborate the nature of the biogenic ZnO NPs. Fourier transform infrared (FTIR) spectroscopy was used in the determination of vibrational properties in 400–4,000 cm^{-1} region. The UV absorption and diffuse reflectance spectra were obtained in 200–800 nm and 0–2,500 nm, respectively. Elemental analysis was carried out using energy-dispersive X-ray spectroscopy. Thermal stability of the NPs was investigated using thermogravimetric analysis (TGA) and their corresponding DTG curve was obtained. Zeta potential was determined using water as dispersant at room temperature. The shape and morphology of the NPs were studied to high resolution (HR)-SEM and HR-TEM at different magnifications. Selected area electron diffraction (SAED) pattern was also obtained. HR-TEM images were processed using ImageJ software for particle size and *d*-spacing determination.

2.4 | Pharmacognostic properties

2.4.1 | Antibacterial activities

Disk diffusion assay as reported previously was used to investigate the antibacterial activity of ZnO NPs (Khalil et al., 2017a; Khalil et al., 2017b) against gram negative and gram-positive bacteria. The gram-positive bacteria were *Staphylococcus epidermidis (ATCC: 14990)* and *Bacillus subtilis (ATCC: 6633)* while gram-negative bacterial strains *Escherichia coli (ATCC: 15224)*, *(ATCC: 4617)*, and *Pseudomonas aeruginosa (ATCC: 9721)*. Prior to the assay, bacterial cultures were standardized by inoculating a loop of culture in 10 ml TSB, followed by incubation for 24 hr at 37°C in a shaking incubator set at 120 rpm. Optical density of the bacterial cultures was adjusted to 0.5 McFarland standards. From the adjusted cultures, bacterial inocula (100 μl) was dispensed on the nutrient agar plate and uniformly spread over the media with sterilized glass rod to make a uniform bacterial lawn. Total volume of 10 μl of each NPs test sample with dilutions (1,000; 500; 250; 150; 100; and 50 μg/ml) were loaded on autoclaved filter paper (6 mm), dried, and placed on the media. For positive control, gentamicin (10 μg) discs were used. Plates were incubated at 37°C for 24 hr. MIC was defined as the least dilution of NPs that inhibited bacterial growth.

2.5 | Antifungal activity

To investigate the antifungal activity, agar well diffusion assay was performed on four pathogenic fungal strains with slight modifications (Khan et al., 2015). *Aspergillus flavus* (FCBP-0064), *Fusarium solani* (FCBP-0187), *Aspergillus niger* (FCBP-0198), and *Aspergillus fumigates* (FCBP-1264) were used for antifungal activity. All the fungal strains were inoculated in a broth and placed in a shaking incubator for 24 hr at 37°C. Assay was performed by adjusting the OD of the broth cultures to 0.5. From standardized cultures, 50 μl of the broth culture was dispensed on the petri plate to make a uniform lawn with sterilized bent glass rod. Then, 20 μl of the test samples were introduced in each well and the test plates were incubated 72 hr at 37°C. The diameter of the zone of inhibition was determined using Vernier caliper. Amp B was used as positive control.

2.6 | ZnO NPs-based nanocosmeceutical cream

Already described procedure was used to prepare ZnO NPs-based cream. Briefly, 6 ml liquid paraffin and 2 g bees wax were introduced to a conical flask and heated at 70°C in water bath to form the oil phase. Then, 0.1 g borax was added to 2 ml distilled water and heated at 50°C to make the aqueous phase. The aqueous and oil phases were mixed and subsequently and ZnO NPs (2 g) were introduced to the mixture and stirred until the mixture was consistent. Biogenic ZnO NPs-based 2% cream formulation was checked for antimicrobial activities. A small chunk from the cream (~100 μl) was placed gently with sterile spatula. Market available antibiotic cream was considered for positive control while the formulation with no ZnO NPs was used as negative control.

2.7 | Antileishmanial potential

MTT cytotoxicity assay was used for determining the inhibition of *Leishmania tropica* (KMH-23) as described previously (Ali et al., 2017; Ovais et al., 2017b). This strain was procured from Khyber Medical University. *Leishmania* promastigotes were used in the study. M199 medium with 10% FBS supplemented through syringe filter was used for culturing parasites to a density of 1×10^6 cells/ml. Various

dilutions (500–31.25 μg/ml) were used in a 96-well plate for cytotoxicity assessment. The negative and positive controls were DMSO and Amp B. The treated parasite cultures with test samples were incubated for 72 hr in a humified CO_2 incubator. Then, 200 μl of the reaction mixture contained 100 μl of the standardized culture, 50 μl of fresh media, and 50 μl of the colloidal NPs suspension in DMSO. Median lethal concentrations (IC50) were determined using Table Curve software. The absorbance was monitored at 540 nm while the percent inhibitory potential was determined as:

$$\%\text{Inhibition} = 1 - \left(\frac{\text{Sample absorbance}}{\text{Positive control absorbance}}\right) \times 100 \quad (2)$$

2.8 | Hemocompatibility

Freshly isolated human blood cells were used in the determination of the compatibility of ZnO NPs with RBC's (Malagoli, 2007). Blood was collected with prior consent in EDTA tubes, centrifuged at 14,000 rpm/5 min for erythrocyte isolation. To the obtained erythrocytes (200 μl), 9.8 ml PBS (pH = 7.2) was introduced to prepare an erythrocyte suspension. In an Eppendorf tube (1.5 ml), 100 μl of the erythrocyte suspension was treated with test samples. The resultant reaction mix was incubated at 35°C for 1 hr and subsequently centrifuged at 10,000 rpm for 10 min. Supernatant was collected and dispensed in the 96-well plate, while absorbance was recorded at 540 nm. The negative and positive controls were DMSO and Triton X-100, respectively. Hemolysis was monitored by using the following formula:

$$\%\text{Hemolysis} = \left\{\frac{\text{Sample}_{ab} - \text{Negative control}_{ab}}{\text{Positive control}_{ab} - \text{Negative control}_{ab}}\right\} \times 100 \quad (3)$$

2.9 | Protein kinase inhibition

Already described standard procedure (Fatima et al., 2015; Yao et al., 2011) was used for protein kinase (PK) inhibition assay of ZnO NPs. *Streptomyces* 85 E strain cultured in ISP4 minimal media was used. Briefly, 100 μl inoculum was introduced from the already standardized culture and spread uniformly over the petri plates for making uniform lawns. Then, 6 mm filter disc impregnated with the test solution was placed carefully on the medium. The inhibitory zones were measured with Vernier calipers after 72 hr incubation at 30°C.

2.10 | Antioxidant assays

Spectrophotometric-based methods for free-radical scavenging using DPPH (Fatima et al., 2015), total reducing power (TRP) (Javed, Usman, Tabassum, & Zia, 2016; Khalil et al., 2018), and total antioxidant capacity (Jafri, Saleem, Ullah, & Mirza, 2017; Rajan, Chandran, Harper, Yun, & Kalaichelvan, 2015) were used to determine the antioxidant potential ZnO NPs. The reagent solution was prepared by dissolving 9.6 mg (DPPH) in 100 ml of methanol. Total volume of 20 μl sample was introduce to 180 μl reagent solution in 96-well plate followed by incubation in dark for 20 min and the results were taken at 517 nm. Equation (2) was used to determine the free-radical scavenging potential.

TRP was investigated using potassium ferricyanide-based method. DMSO and ascorbic acid were used as negative and positive controls while results were taken at 630 nm and expressed as ascorbic acid equivalents per mg. TAC was determined using phosphomolybdenum method. Results were taken at 695 nm and expressed as ascorbic acid equivalents per mg. The final concentrations of the test sample were 100–25 μg/ml. The antioxidant assays were performed in 96-well plate.

2.11 | Catalytic dye degradation

Previously described method was used dye degradation activity of the ZnO NPs (Singh et al., 2018). For catalytic degradation, the crystal violet dye (CVD) was studied under four different parameters, that is, with and without sunlight irradiation, with UV and the sonophotocatalytic degradation. Then, 5 mg CVD was added to 250 ml distilled water for preparing dye solution. In addition, 60 mg ZnO NPs were introduced to the solution followed by stirring in an orbital shaker for 20 min in dark. A control sample of CVD with no treatment was prepared and kept under similar conditions. To investigate the photocatalytic degradation, the test solution was kept under sunlight and in dark with periodic stirring. To study the effect of UV, test reaction aliquot was kept under UV illumination. The UV illuminator was equipped with 6 W UV lamp 6GT5 (Sankyo Denki, Japan). Sonophotocatyltic degradation was studied by placing the test aliquots under sonication. The UV readings were determined by taking 1 ml of the suspension, followed by centrifugation at 5,000 rpm for 15 min to obtain a clean supernatant after every 2 hr. The experiment was performed in the month of June with an average daylight ~11–12 hr and an average temperature of 38°C. The catalytic degradation of CVD was determined using the following formula:

$$\%\text{Degradation} = \left(C_0 - C/C_0\right) \times 100 \quad (4)$$

whereas C_0 is the initial concentration of dye and C is the dye concentration after specific time interval.

3 | RESULTS AND DISCUSSION

3.1 | Biosynthesis and characterization ZnO NPs

Physical or chemical methods to fabricate NPs are often accompanied by disadvantages like cost, energy consumption, and toxicity. Recently, it was reported that toxic chemicals can remain adhered to the NPs which limits their use for biomedical applications. In

comparison, green synthesis does not possess such drawbacks and therefore used here. Aqueous extracts of *F. indica* were successfully used as reducing and stabilizing agents for the biosynthesis of ZnO NPs. *F. indica* possess a rich phytochemistry and the phytochemicals are involved in the synthesis of NPs. Some of the phytochemicals reported from *F. indica* are Kaempferol, Quercetin, Glucopyranosides, Saponins, Triterpenoid, Coumarins, Alkaloids, Flavonoids, and Tannins (Bagban et al., 2012). Such phytochemicals actively allow the process of reduction, followed by capping and stabilizing the NPs. A general study layout indicating in the process of biosynthesis is described in Figure 1.

Figure 2 indicates the XRD pattern of the ZnO_A and ZnO_S NPs annealed at 500°C. The Bragg peaks were found consistent with "JCPDS pattern 00–036–1451" which corresponds to the single and pure hexagonal phase of zincite or chinse white form of ZnO. The sharp nature of the peaks indicates a high degree of crystallinity of the NPs. From the JCPDS card, the lattice constants were deduced as $<a_{exp.}> = 3.24982$ and $<c_{exp.}> = 5.20661$ Å. The grain size of the NPs was determined to be 23.4 nm (ZnO_A) and 41.2 nm (ZnO_S) using Debye–Scherrer approximation. Major values deduced from XRD spectra are indicated in Table 1. No other peaks pertaining to the impurities were found which indicate the single-phase purity of the NPs.

The inset of Figures 3 and 4 indicates various analyses performed on the ZnO_A and ZnO_S NPs. Figures 3a–g and 4a–g indicate different HR-TEM images of the NPs at different magnifications. By close observation, the shape of the ZnO_A NPs and ZnO_S NPs appears to possess a plate-like morphology. The individual particle size calculated for ZnO_A NPs and ZnO_S NPs are found to be ~100 and ~50 nm, respectively. Figures 3d and 4d indicate the HR-TEM images with lattice fringes clearly visible which underlines the crystalline nature of the NPs. The *d*-spacing was calculated to be 0.25 and 0.3 nm for ZnO_A and ZnO_S NPs, respectively. The HR-SEM images of the biogenic NPs are indicated in Figures 3e and 4e. The SAED pattern for both the ZnO_A and ZnO_S NPs reveals a spotty ring pattern which indicates the crystalline nature of the particles. The EDS spectra indicated an intense peak of Zn and O elements. However, other elements were also found which may be attributed to the extracts-based synthesis being rich in mineral elements. The EDS results are indicated in Figures 3g and 4g.

The FTIR spectra of the as-synthesized ZnO_A NPs and ZnO_S NPs are indicated in Figure 5a,b, respectively. Major IR absorptions were singled out. The spectra indicate sharp fingerprint vibrations at ~450 cm^{-1} which is attributed to the characteristic Zn—O stretching vibration (Babu, Reddy, Sujatha, Reddy, & Mallika, 2013). The other common peaks centered at ~1,550 cm^{-1} can be attributed to C—O stretching vibrations. Other common functional groups are centered on ~3,200 cm^{-1} (ZnO_S) and 3,400 cm^{-1} (ZnO_A) which represents the alcoholic and phenolic phytochemicals. Some of the distinctive vibrations can attributed to the rich phytochemistry of the aqueous extracts of *F. indica* which has played a role in reducing and stabilizing of the NPs. It is interesting to note that, these functional groups remain attached to the NPs even after high temperature thermal annealing. The detailed assignment of the functional groups can be found in Figure 5a,b. The UV absorption spectra of the NPs and plant extracts are indicated in Figure 5c. The characteristic SPR peak of nanoscaled ZnO NPs can be observed at 378 nm (ZnO_S) and 371 nm (ZnO_A) which is in agreement with the earlier studies (Zak, Razali, Abd Majid, & Darroudi, 2011). The band gap was calculated as 3.2 and 3.3 eV for ZnO_S and ZnO_A, respectively. The smaller band gap can be attributed to various factors like planer defects, twin boundaries, stacking faults, and intrinsic defects like zinc and oxygen vacancies. The band gap of the particle increases when the size of the particle decreases which is also indicated from our results (Dejene et al., 2011; Jangir, Kumari, Kumar, Kumar, & Awasthi, 2017). Generally, the ZnO_S particles possessed a large size distribution and therefore small band gap as compared to the ZnO_A particles which possessed a small size particle distribution. Figure 5d indicates the diffuse reflectance spectra of the as-synthesized NPs. Strong reflectance was observed for the ZnO_A NPs after 400 nm which is in agreement with some of the earlier studies. The inset Figure 6a,b shows thermogravimetric curves (TGA) and their corresponding first-order derivative (DTG) of the NPs in the range of 0–900°C. The thermal analysis indicated one small weight loss events at ~190°C and a large weight loss event at ~659°C for ZnO_A NPs. The first event can be attributed to desorption and loss of physically or chemically adsorbed moisture and alcohols (Dejene et al., 2011). The second event can be attributed to the loss and decomposition of phytochemicals and carbon-related components, while the second event can be attributed to the decomposition of the charred products (Al-Shabib et al., 2016). For ZnO_S NPs, three weight loss events were observed at ~386, 560, and 723°C. These decomposition events can be attributed to the loss of moisture or other phytochemical components. The zeta potential of the NPs was carried out after 6 months of storage. The deduced zeta potential values are indicated in Table 1. The results indicated a negative zeta potential value −0.551 and −1.01 mV for ZnO_A NPs and ZnO_S NPs, respectively. This zeta potential value indicated the presence of relatively weaker repulsive forces and a slight tendency toward aggregation. The measurement of zeta potential is based on the movement of particles under electric field. Surface charge of the particles and local environment plays a definitive role in the measurement (Chaudhuri & Malodia, 2017).

3.2 | Antimicrobial activities

In antibacterial assay, all the ZnO NPs showed inhibition against the bacterial strains using disc diffusion method carried out at different concentrations (1,000–50 μg/ml). It was found that ZnO_A NPs were most effective against *B. subtilis* (MIC 50 μg/ml) and *E. coli* (MIC 100 μg/ml) and least effective against *Klebsiella pneumonia* and *P. aeruginosa* with MIC of 250 μg/ml each. The ZnO_S NPs were found to be most effective against *K. pneumonia* (Table 2). The antibacterial properties of ZnO NPs have been well documented in earlier reports (Lingaraju et al., 2016). The ROS generation is considered as a primary mechanism that imparts the antimicrobial nature to ZnO NPs. ROS's

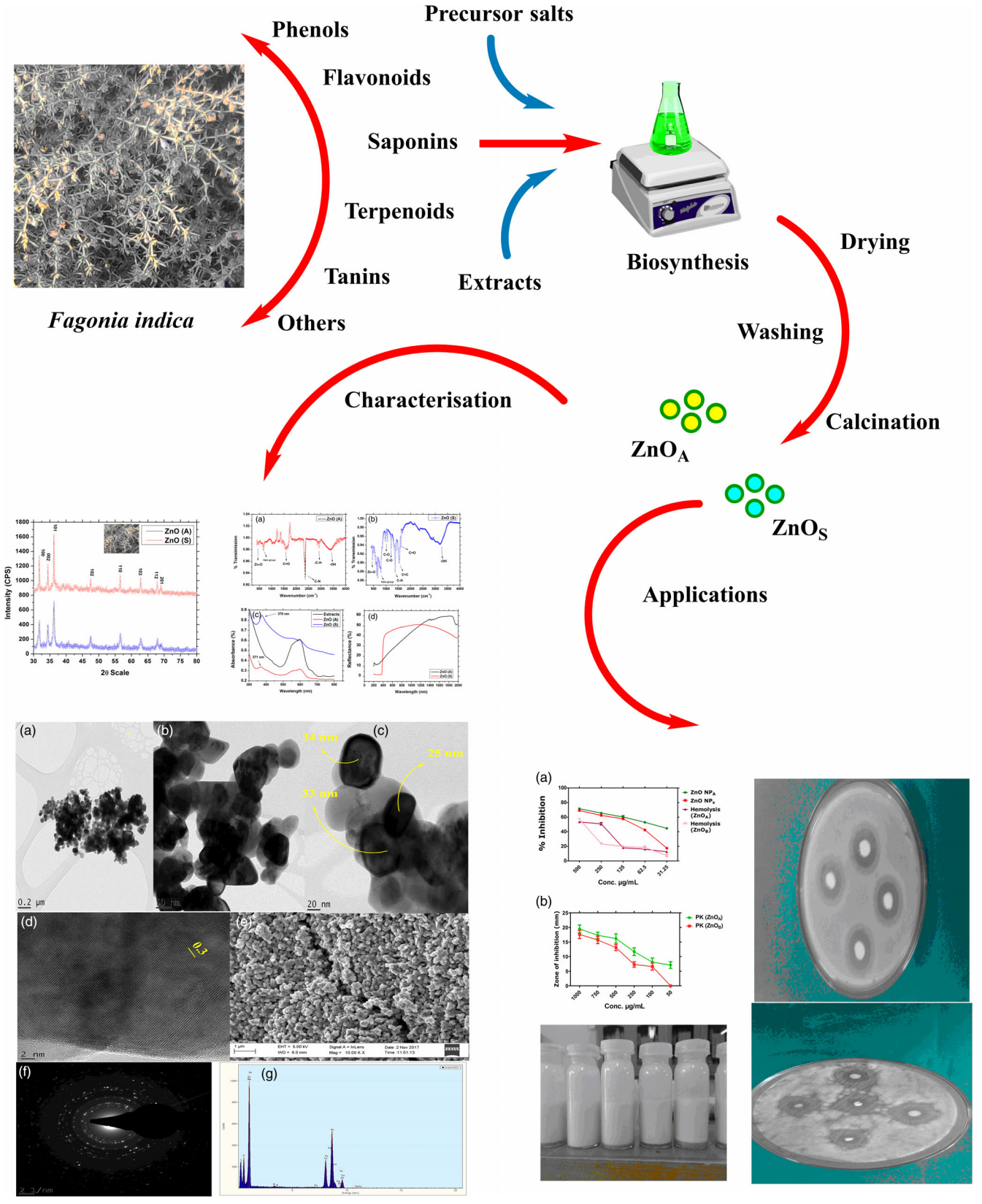

FIGURE 1 Study scheme from biosynthesis to applications

like H_2O_2 can penetrate inside the organism to initiate the genotoxic effects. In a recent study, on ZnO NPs, ROS generation was considered to be a small factor in the antimicrobial nature while alteration of carbohydrate metabolism was found to be the primary cause of killing of methicillin resistant *Staphylococcus aureus* (Kadiyala, Turali-Emre, Bahng, Kotov, & VanEpps, 2018). Surface defects in the NPs are also

considered a reason for the antibacterial activity. Several researchers have attempted to examine the antimicrobial potential of ZnO NPs. Impressive antibacterial potential against gram-positive and gram-negative bacterial strains are reported, which are in agreement with the earlier findings (Raja et al., 2018).

Antifungal potential of *F. indica* mediated nanocrystals was measured using well diffusion assay and the results are indicated (Table 3). Antifungal activity was investigated for the stock concentrations (1,000–50 μg/ml) against four pathogenic fungal strains. Our results suggested inhibition of the tested strains at higher concentrations; however, the inhibition was insignificant relative to positive control Amp B. Among the tested strains, *F. solani* was investigated to be the most susceptible strain in case of ZnO_A NPs and *A. niger* in case of ZnO_S. Along with the generation of reactive oxygen species, ZnO NPs are also reported to interfere with the hyphae and spores of the fungus, thereby retarding or inhibiting their growth (He, Liu, Mustapha, & Lin, 2011; Lipovsky, Nitzan, Gedanken, & Lubart, 2011). In general, a dose-dependent inhibition is reported.

The antibacterial and antifungal potential of the ZnO NPs was further confirmed through the nano-based cosmeceutical cream formulation. Then, 2% of the cream revealed impressive results as indicated in Figure 7.

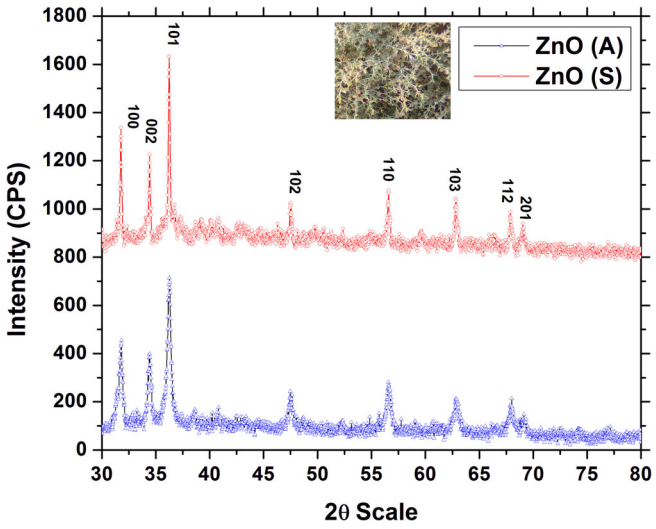

FIGURE 2 XRD spectra of *Fagonia indica* mediated zinc oxide nanoparticles (ZnO NPs); Letters (A) and (S) denote different precursor salts

3.3 | Antileishmanial activity

Leishmaniasis is categorized as a neglected tropical disease, endemic to 98 countries. About 350 million people across the globe face an immediate threat from the parasite. In addition, the current medications are insufficient in treating *Leishmania*, while the gold standard treatments like antimonials are getting resistant at alarming rates (Abamor, 2017; Ouellette et al., 2008). Recently, scientists are looking toward the nano-based interventions for treating *Leishmania*. Some studies on chemically synthesized ZnO NPs revealed impressive results. Chemically or biologically synthesized metal oxides has already been demonstrated to have potential antileishmanial activities (Nadhman, Khan, Nazir, et al., 2016; Nadhman, Sirajuddin, Nazir, & Yasinzai, 2016). The axenic promastigote cultures of *L. tropica* were studied using ZnO_A and ZnO_S NPs in the concentration range of 500–31.25 μg/ml. A dose-dependent response is concluded. The parasite was inhibited up to 71.64 and 69.12% for ZnO_A and ZnO_S NPs at 500 μg/ml. The median lethal concentration (IC_{50}) calculated using Table Curve, indicated ZnO_A NPs as much more effective as compared to ZnO_S. The IC_{50} values were 48 and 83 μg/ml for ZnO_A and ZnO_S NPs. The results are indicated in Figure 8a. These results indicate a good inhibitory potential of *F. indica* mediated ZnO_A and ZnO_S. Using the same method, protocol and strain, earlier we found that the ZnO using *Sageretia thea* indicated IC_{50} value of 6.27 μg/ml, which is

TABLE 1 Zeta potential measurements of the ZnO NPs

	Mean	
Parameters	**ZnO_A**	**ZnO_S**
Zeta potential [62]	−0.551	−1.01
Zeta deviation [62]	8.58	9.87
Conductivity (mS/cm)	1.98	3.57
Result quality	Good	Good

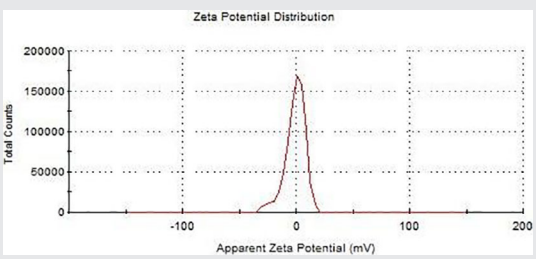

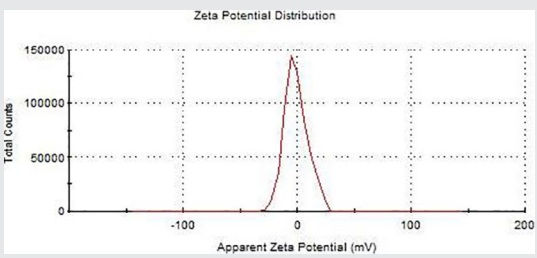

Abbreviations: NPs, nanoparticles; ZnO, zinc oxide.

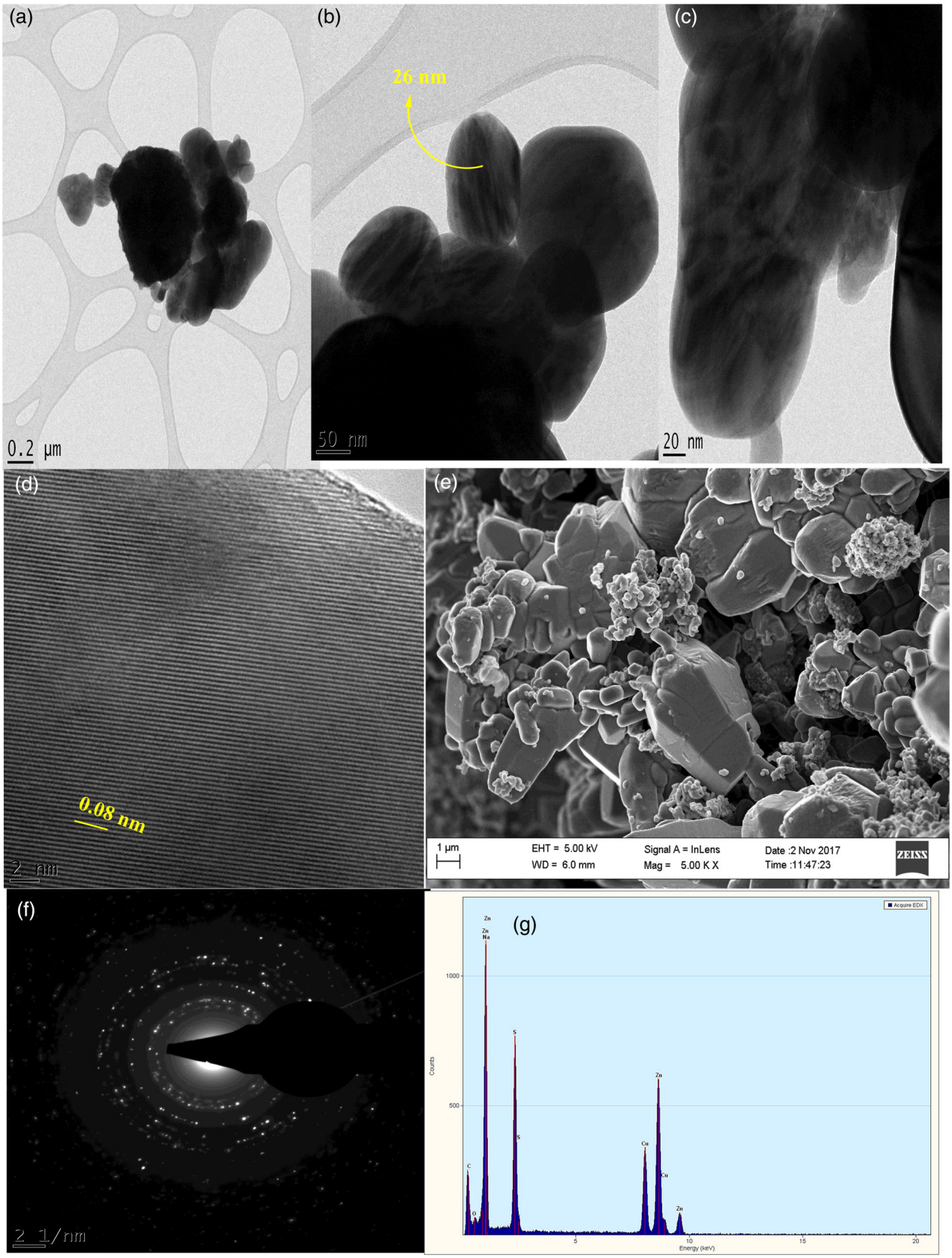

FIGURE 3 (a–d) Various high resolution (HR)-TEM images of *Fagonia indica* mediated zinc oxide nanoparticles (ZnO NPs) using zinc acetate as precursor; (e) their HR-SEM image; (F) their selected area electron diffraction (SAED); and (g) energy-dispersive X-ray spectroscopy (EDX)

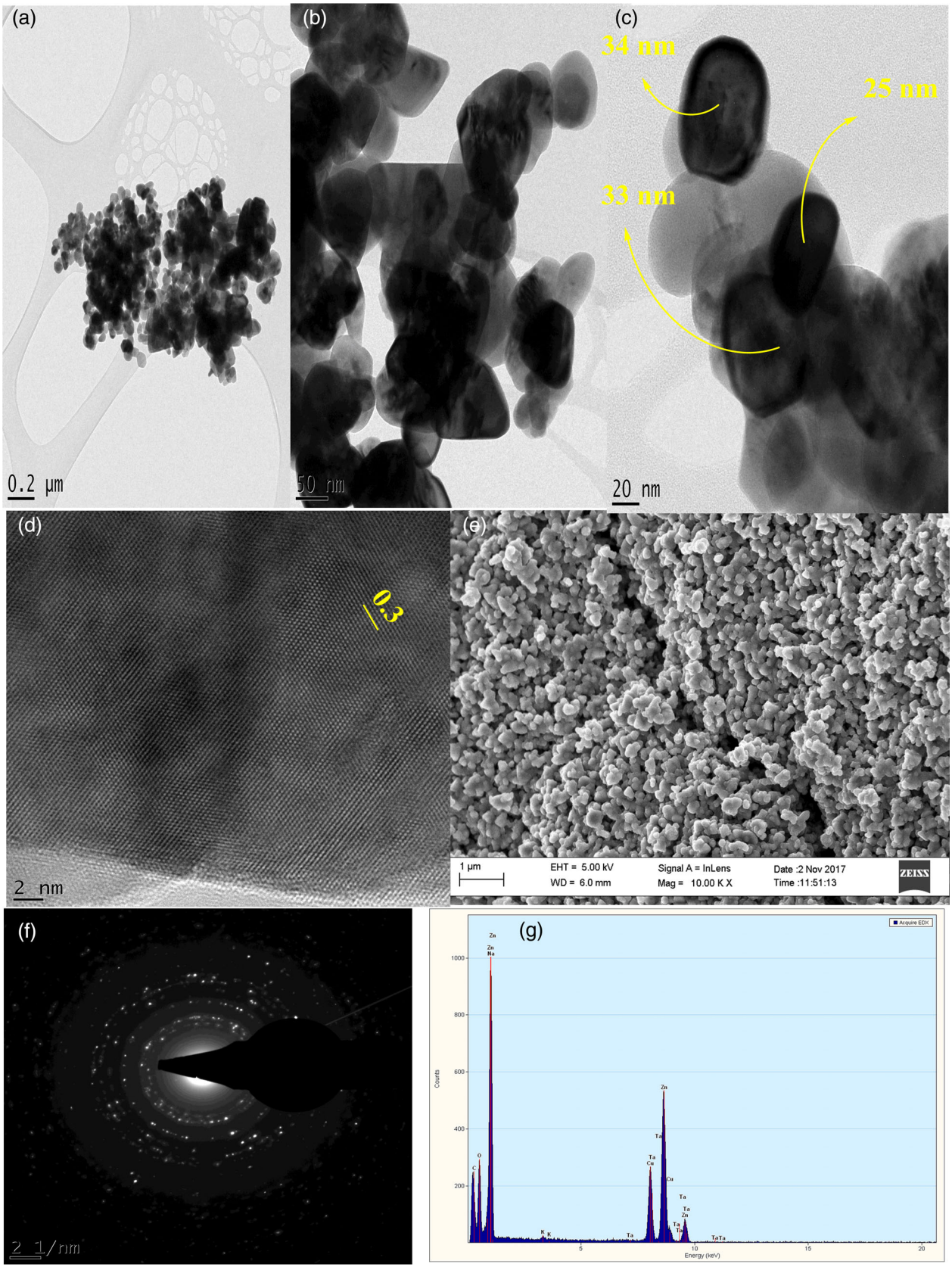

FIGURE 4 (a–d) Various high resolution (HR)-TEM images of *Fagonia indica* mediated zinc oxide nanoparticles (ZnO NPs) using zinc sulfate as precursor; (e) their HR-SEM image; (f) their selected area electron diffraction (SAED); and (g) energy-dispersive X-ray spectroscopy (EDX)

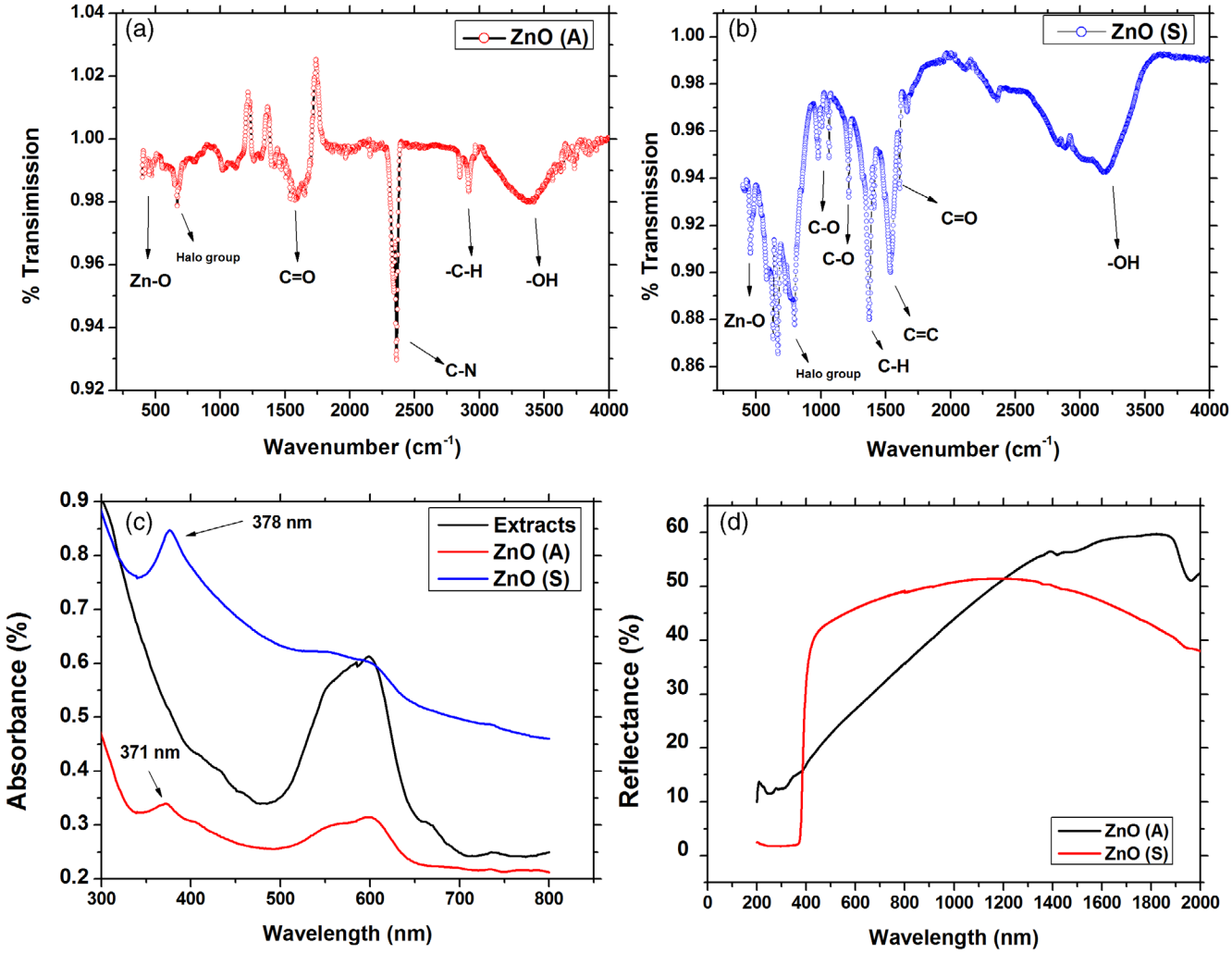

FIGURE 5 (a) Fourier transform infrared (FTIR) spectra of the zinc oxide nanoparticles (ZnO NPs) biosynthesized using zinc acetate as precursor; (b) FTIR spectra of the ZnO NPs biosynthesized using zinc sulfate as precursor; (c) UV absorption spectra; and (d) diffuse reflectance spectra

significantly lower than the IC_{50} in the present study (Khalil et al., 2017a; Khalil et al., 2017b). Therefore, the nature of the plant used can have a definitive effect on the biological activities of the NPs.

3.4 | Hemocompatibility

To assess the effect of precursor's salts on the biocompatible nature of NPs, hemolysis was performed in the concentration range of 500–31.25 μg/ml. The standard comparison was drawn with the American Society for Testing and Materials which suggest that with hemolysis <2% nonhemolytic, 2–5% slightly hemolytic and >5% are hemolytic (Aula et al., 2014). It can be observed from Figure 8a, that a hemolysis is reported in a dose-dependent manner which gradually decreases as the concentration is lowered, that is, from hemolytic to nonhemolytic as a function of concentration of the sample. The IC_{50} was determined as 364 and 458 μg/ml for ZnO_A and ZnOs NPs, respectively. Among the tested concentration, both types of the NPs suggested hemolysis up to 31.25 μg/ml. An interesting relation is also established with reference to the particle size and % hemolysis. The hemolysis caused by ZnO_A NPs at highest concentration appears less than the treatment of ZnO_S NPs, indicating the size-dependent toxicity.

3.5 | PK inhibition

Figure 8b shows the ability of biogenic ZnO NPs to inhibit PK enzymes. PKs are basically accountable for the phosphorylation of tyrosine, serine, and threonine residues, which serve as a pivotal regulatory process for metabolism, cellular differentiation/proliferation, and apoptosis. Deregulated phosphorylation can induce genetic abnormalities leading to tumorigenesis. Therefore, inhibition of PKs is considered a popular strategy to inhibit tumorigenesis (Waters et al., 2002). PK phosphorylation plays an important role in the establishment of hyphae in

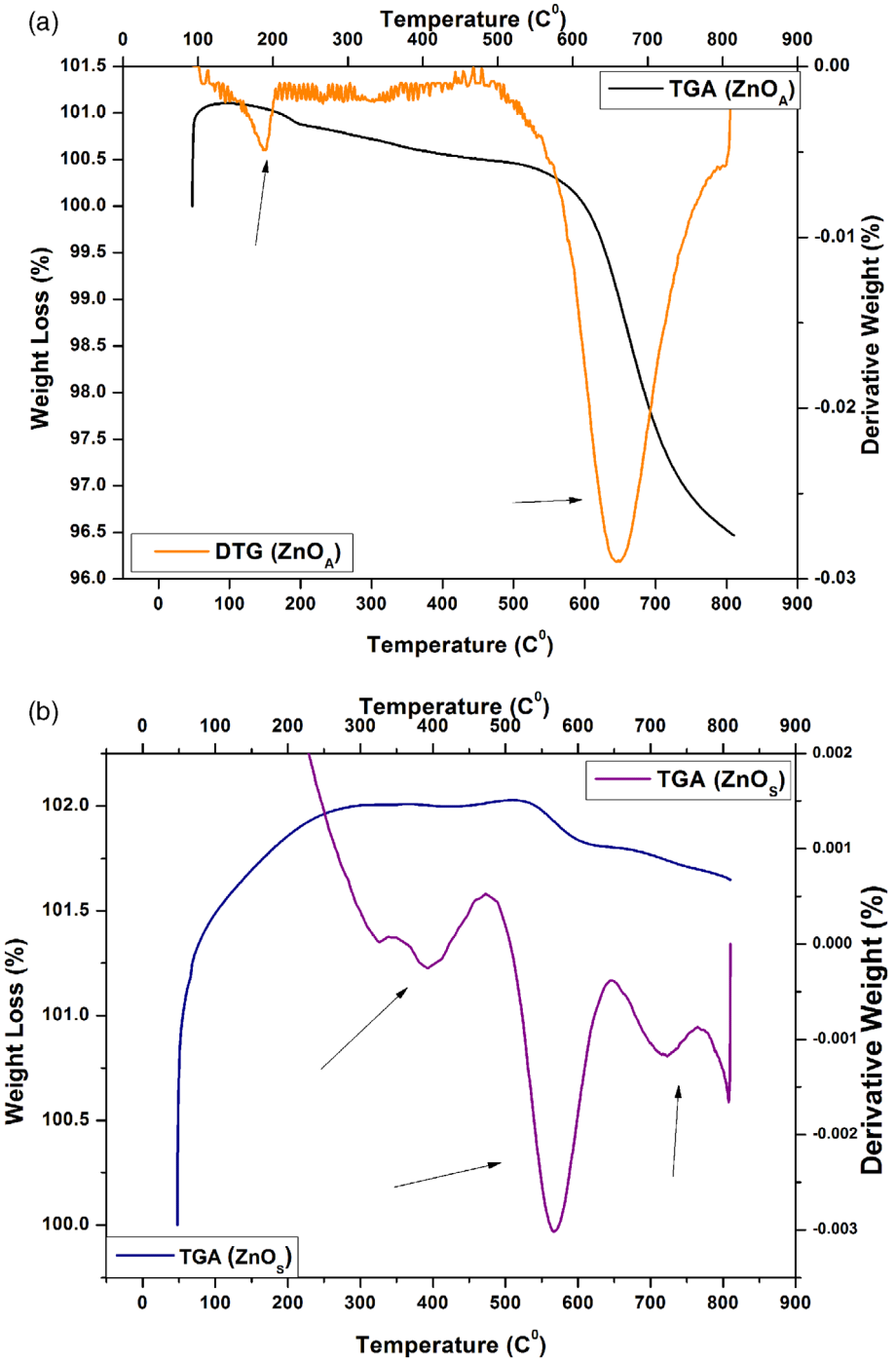

FIGURE 6 Thermogravimetric analysis (TGA)–DTG curves of *Fagonia indica* mediated zinc oxide nanoparticles (ZnO NPs); (a) using zinc acetate and (b) using zinc sulfate

Streptomyces fungal strains, and the same principal is explored to determine the PK inhibition activity. *Streptomyces* 85E strain has been widely employed to investigate medicinal compounds for investigation of the PK inhibition (Waters et al., 2002). *F. indica* mediated NPs indicated significant PK inhibition potential. The ZnO_A and ZnO_S NPs effectively inhibited the PK enzyme from 1,000 to 100 μg/ml, while the ZnO_A NPs were also effective at 50 μg/ml and indicated 7.1 mm zone of inhibition. The inhibitory zones appeared as 19.5 ± 1.32 and 17.6 ± 1.4 mm at 1,000 μg/ml, while gradually lowered with the decrease in concentration. Therefore, a potential signal transduction inhibitor has been identified in the form of ZnO NPs, which can be explored for anticancer features.

3.6 | Antioxidant potential

The inset of Figure 9 indicates various antioxidant activities of the *F. indica* mediated NPs. Our results indicate moderate to good DPPH free-radical scavenging potential for the ZnO_A and ZnO_S NPs. DPPH scavenging activity involve the formation of a yellow molecule

TABLE 2 The antibacterial activity of ZnO NPs of zinc acetate and zinc sulfate extracts against pathogenic bacterial and their inhibitory zones

	Gram positive				Gram negative					
Plant extract	*Bacillus subtilis* (ZOI)	MIC (μg/ml)	*Staphylococcus epidermis* (ZOI)	MIC (μg/ml)	*Pseudomonas aeruginosa* (ZOI)	MIC (μg/ml)	*Klebsiella pneumonia* (ZOI)	MIC (μg/ml)	*Escherichia coli* (ZOI)	MIC (μg/ml)
ZnO_A	6.6 ± 1.1***	50	9.6 ± 1.5***	150	8.5 ± 0.9***	250	7.1 ± 1.0***	250	9.2 ± 1.7***	100
ZnO_S	7.1 ± 0.7***	150	8.2 ± 1.5***	150	9.1 ± 1.5***	150	7.4 ± 1.2***	100	7.4 ± 1.0***	150
Gentamicin	21.8 ± 1.8		17.6 ± 1.4		16.7 ± 1.09		17.2 ± 1.23		16.4 ± 1.51	

Note: Inhibition zones includes diameter of disc (6 mm). Samples are analyzed in triplicate (mean ± *SD*). ***Highly significant, **slightly significant, *nonsignificant difference from control at $p < .05$ by one-way ANOVA. No activity or zones less than 10 mm were not considered for MIC.
Abbreviations: ANOVA, analysis of variance; NPs, nanoparticles; ZnO, zinc oxide; ZOI, zone of inhibition (mm).

TABLE 3 Antifungal activity of ZnO NPs of zinc acetate and zinc sulfate extracts against pathogenic fungi and their inhibition zones

Samples	*Fusarium solan* (ZOI)	MIC (μg/ml)	*Aspergillus flavus* (ZOI)	MIC (μg/ml)	*Aspergillus fumigatus* (ZOI)	MIC (μg/ml)	*Aspergillus niger* (ZOI)	MIC (μg/ml)
ZnO_A	9.9 ± 0.7***	100	7.2 ± 1.0***	250	6.4 ± 1.1***	250	8.3 ± 1.1***	150
ZnO_S	8.3 ± 0.8***	250	6.8 ± 1.2***	250	8.4 ± 1.15***	500	9.2 ± 0.642***	100
Amphotericin B	17.6 ± 1.4		16.7 ± 1.09		17.2 ± 1.23		16.4 ± 1.51	

Note: Samples are analyzed in triplicate (mean ± *SD*). ***Highly significant, **slightly significant, *nonsignificant difference from control at $p < .05$ by one-way ANOVA. No activity or zones less than 10 mm were not considered for MIC.
Abbreviations: ANOVA, analysis of variance; NPs, nanoparticles; ZnO, zinc oxide; ZOI, zone of inhibition (mm).

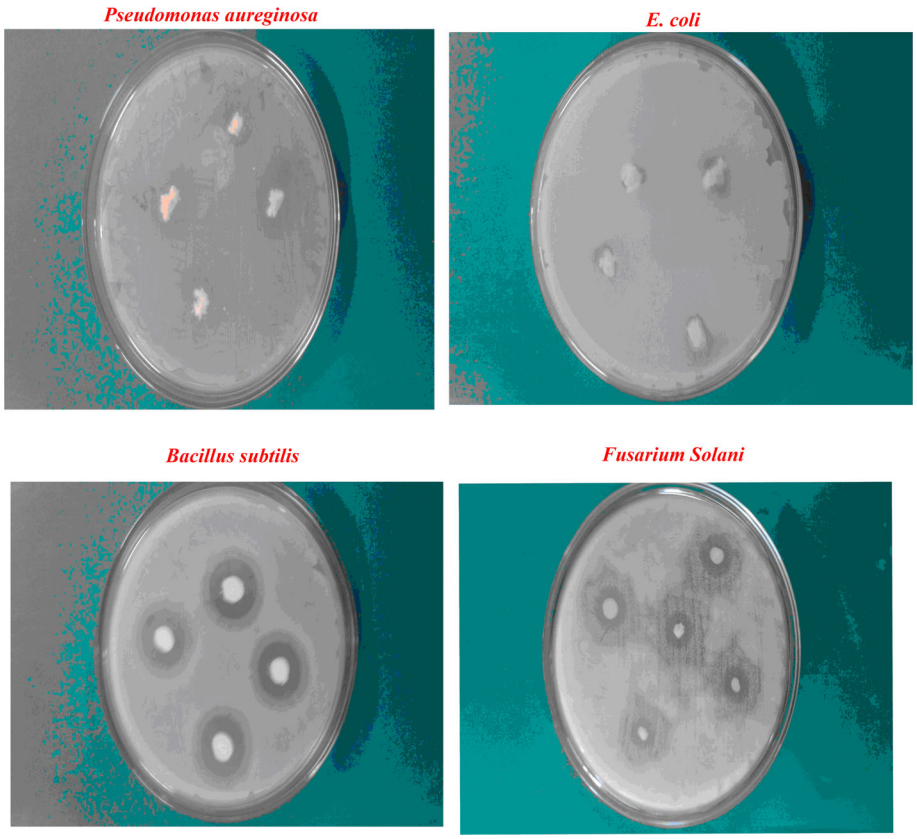

FIGURE 7 Antimicrobial potential of the 2% zinc oxide nanoparticles (ZnO NPs)-based cream

(diphenyl picrylhydrazine), when DPPH moiety is accepts electron or hydrogen from and get reduced. Our result indicated 66.8 and 77.2% free-radical scavenging potential at the highest tested concentration, that is, 500 μg/ml for ZnO_A and ZnO_S NPs, respectively, while gradually reduced as the concentration of the test sample was decreased. Furthermore, our results indicate that ZnO_S NPs were more effective

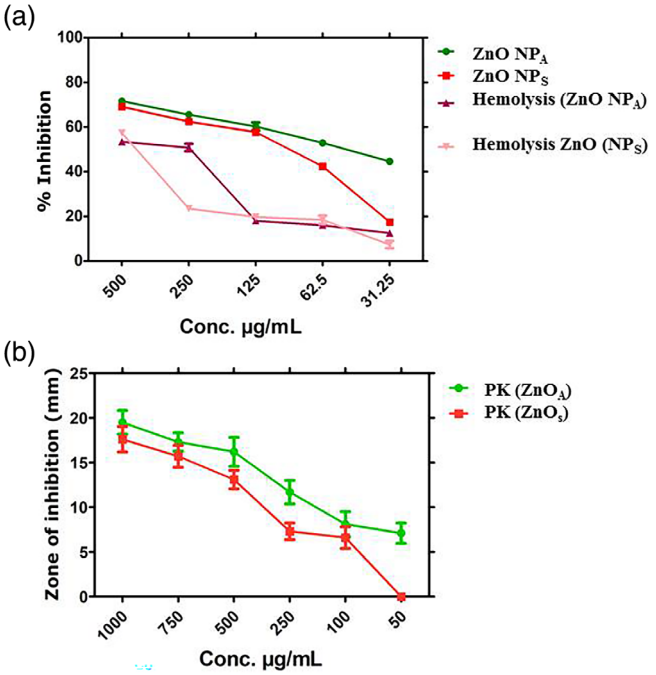

FIGURE 8 (a) Antileishmanial and hemolytic activities of *Fagonia indica* mediated zinc oxide nanoparticles (ZnO NPs) and (b) their protein kinase inhibition

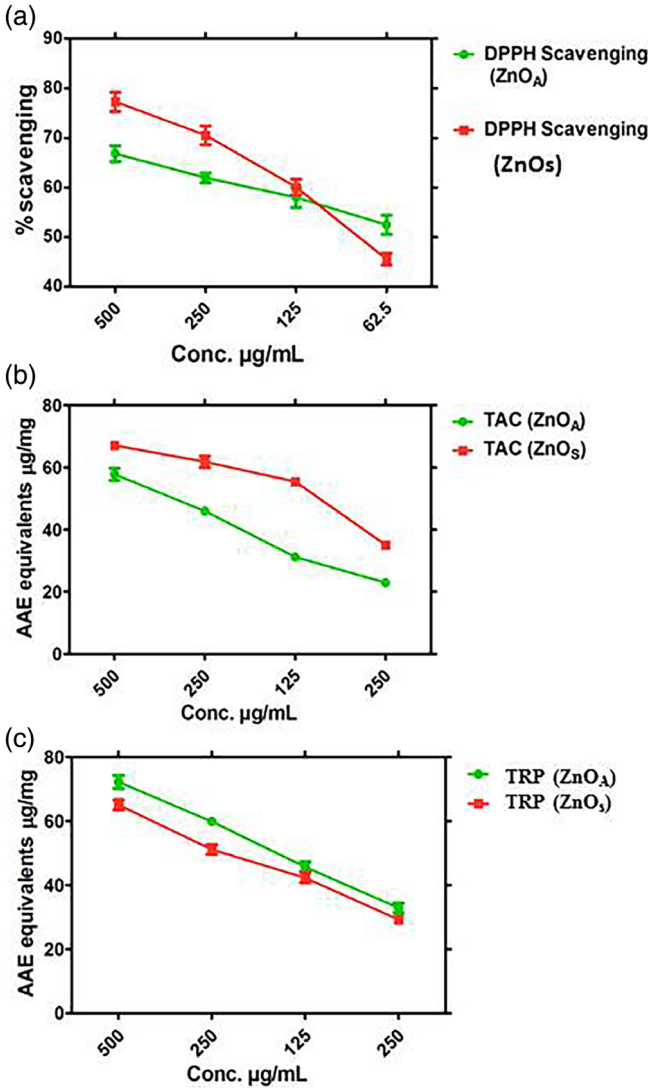

FIGURE 9 Antioxidant potential of the *Fagonia indica* mediated zinc oxide nanoparticles (ZnO NPs); (a) DPPH free-radical scavenging, (b) total antioxidant capacity, and (c) total reducing power

in DPPH radical scavenging as compared to the ZnO_A NPs. The results are in agreement with earlier findings (Rajakumar, Thiruvengadam, Mydhili, Gomathi, & Chung, 2018). The results are indicated in Figure 9a. The antioxidant potential was further assessed by means of TAC (Alegria et al., 2018). TAC is performed to assess the quenching capacity of the tested materials toward ROS. Figure 9b indicates the TAC results of the biogenic NPs expressed as AAE equivalents µg/mg. Herein also, moderate to good TAC for the NPs are reported while ZnOS NPs were more effective relative to ZnO_A NPs. TAC is based on the conversion of Mo to Mo (Lokesh et al., 2016) subsequently followed by the formation of greenish Mo-phosphate complex having maximum absorption at 695 nm. The maximum value in terms of AAE equivalents was obtained at 500 µg/ml for ZnO_A and ZnO_S NPs, that is, 57.7 and 67.09 AAE eq µg/mg, respectively. A steady decrease in TAC is observed by lowering the concentration. To further verify the antioxidant potential of the as-synthesized NPs, TRP assay was performed as indicated in Figure 9c. This assay is dependent on reductones which are involved in the antioxidation potential by donating an H-atom resulting in the breakage of the free-radical chain. The TRP of ZnO_A NPs is reported to be slightly higher as compared to the ZnO_S NPs. The maximum reducing potential (72.2%) was reported for ZnO_A NPs at 500 µg/ml. Overall, the results of the antioxidant activity indicate a good antioxidant potential of the *F. indica* mediated NPs. It can be suggested that some antioxidant phytochemicals in *F. indica* were responsible for capping of the NPs which may have contributed to the good antioxidant activities of the NPs. The results are in agreement with some of the earlier findings on biogenic ZnO NPs.

Variation and disagreement in relative to other studies can be due to numerous factors like experimental conditions (seasonal variation, location, and humidity), while other factors like method of NP synthesis, plant used, and size of the NPs can be significant factors.

3.7 | Dye degradation

The as-synthesized NPs were investigated for catalytic degradation of CVD under different conditions. In most of the cases, the percent degradation was higher in the first 2 hr of the experiment. The degradation of CVD up to ~60% was achieved using ZnO_A NPs after 10 hr while 51% for ZnO_S NPs under sunlight radiation. The order of degradation that was revealed by the ZnO_A NPs was degradation in sunlight > degradation in dark > degradation in UV > degradation under sonication (sonophotocatalytic). The pattern followed by

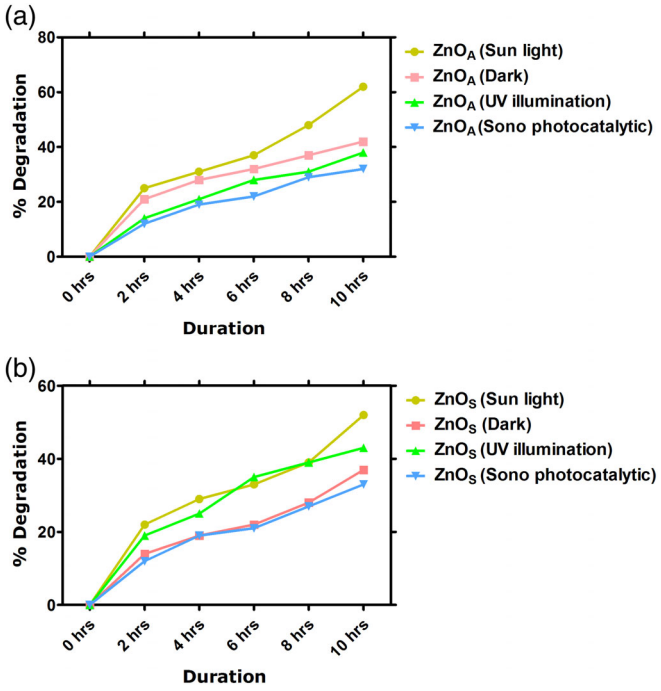

FIGURE 10 Dye degradation potential of *Fagonia indica* mediated zinc oxide nanoparticles (ZnO NPs); (a) using zinc acetate as precursor and (b) using zinc sulfate as precursor

the ZnO_S NPs is, however, different, that is, degradation in sunlight > degradation in UV > degradation in dark > degradation under sonication (sonophotocatalytic). The degradation potential of dyes using ZnO NPs is well established. The basic mechanism involved is the excitation of electrons from valence band (VB) to condition band (Azizi et al., 2016) of a wide band gap semiconductor leaving a positive hole in the VB. The electrons and holes serve as charge carriers to induce redox reactions in the adsorbed molecular thus allow degradation of the dye. The variation in percent degradation by ZnO NPs may be due to size, shape, and different surface functional groups as indicated by FTIR. The results of dye degradation experiment under different conditions are indicated in Figure 10a,b.

4 | CONCLUSION

Physical, biological, and catalytic nature of *F. indica* mediated ZnO NPs under different conditions are established and were studied with reference to the precursor salt used. Our results indicated varying nature of the ZnO NPs with reference of the precursor salt. The overall biological properties of both types of NPs were impressive; however, the acetate-based ZnO NPs indicated a slightly better biological as well as catalytic properties. Excellent antibacterial, antileishmanial, antioxidant, and PK inhibition activities are reported. In addition, the nanocosmeceutical formulation revealed excellent antifungal properties. Furthermore, the blood compatibility results indicated a toxicity toward RBC's at higher concentrations and the degree of compatibility increased at lower tested concentrations. Therefore, further studies on the compatibility of these NPs at lower concentrations should be carried out and should not be used unless their safety is established. The catalytic degradation of CVD under different conditions is also established. To conclude, recommend in vivo studies on the toxicity in animal models, and for once, the safety is established, only then the NPs can be used clinically.

ACKNOWLEDGMENTS

The authors are thankful to the UNESCO UNISA Africa Chair in Nanosciences and Nanotechnology, Higher Education Commission, Pakistan, and Pakistan Academy of Sciences.

CONFLICT OF INTEREST

The authors declare no conflicts of interest.

DATA AVAILABILITY STATEMENT

The authors declare that any needed data that can support the findings of this study are available from the corresponding author upon reasonable request.

ORCID

Safia Hameed https://orcid.org/0000-0002-5052-7172
Javed Iqbal https://orcid.org/0000-0002-9032-2622
Banzeer Ahsan Abbasi https://orcid.org/0000-0003-3036-4481

REFERENCES

Abamor, E. S. (2017). Antileishmanial activities of caffeic acid phenethyl ester loaded PLGA nanoparticles against *Leishmania infantum* promastigotes and amastigotes in vitro. *Asian Pacific Journal of Tropical Medicine*, *10*(1), 25–34.

Abbasi, B. A., Iqbal, J., Khan, Z., Ahmad, R., Uddin, S., Shahbaz, A., & Mahmood, T. (2020). Phytofabrication of cobalt oxide nanoparticles from *Rhamnus virgata* leaves extract and investigation of different bioactivities. *Microscopy Research and Technique*, *84*(2), 192–201.

Abbasi, B. A., Iqbal, J., Kiran, F., Ahmad, R., Kanwal, S., Munir, A., & Mahmood, T. (2020). Green formulation and chemical characterizations of *Rhamnella gilgitica* aqueous leaves extract conjugated NiONPs and their multiple therapeutic properties. *Journal of Molecular Structure*, *1218*, 128490.

Abbasi, B. A., Iqbal, J., Mahmood, T., Khalil, A. T., Ali, B., Kanwal, S., & Ahmad, R. (2018). Role of dietary phytochemicals in modulation of miRNA expression: Natural swords combating breast cancer. *Asian Pacific Journal of Tropical Medicine*, *11*(9), 501.

Abbasi, B. A., Iqbal, J., Mahmood, T., Qyyum, A., & Kanwal, S. (2019). Biofabrication of iron oxide nanoparticles by leaf extract of *Rhamnus virgata*: Characterization and evaluation of cytotoxic, antimicrobial and antioxidant potentials. *Applied Organometallic Chemistry*, *33*(7), e4947.

Abbasi, B. A., Iqbal, J., Nasir, J. A., Zahra, S. A., Shahbaz, A., Uddin, S., & Mahmood, T. (2020). Environmentally friendly green approach for the fabrication of silver oxide nanoparticles: Characterization and diverse biomedical applications. *Microscopy Research and Technique*, *83*(11), 1308–1320.

Abbasi, B. A., Iqbal, J., Zahra, S. A., Shahbaz, A., Kanwal, S., Rabbani, A., & Mahmood, T. (2020). Bioinspired synthesis and activity characterization of iron oxide nanoparticles made using *Rhamnus Triquetra* leaf extract. *Materials Research Express*, *6*(12), 1250e7.

Ahmad, M., Qureshi, R., Arshad, M., Khan, M. A., & Zafar, M. (2009). Traditional herbal remedies used for the treatment of diabetes from district Attock (Pakistan). *Pakistan Journal of Botany*, *41*(6), 2777–2782.

Alegria, E. C., Ribeiro, A. P., Mendes, M., Ferraria, A. M., Do Rego, A. M. B., & Pombeiro, A. J. (2018). Effect of phenolic compounds on the synthesis of gold nanoparticles and its catalytic activity in the reduction of nitro compounds. *Nanomaterials*, *8*(5), 320.

Ali, A., Ambreen, S., Javed, R., Tabassum, S., Ul Haq, I., & Zia, M. (2017). ZnO nanostructure fabrication in different solvents transforms physiochemical, biological and photodegradable properties. *Materials Science and Engineering: C*, *74*, 137–145.

Al-Shabib, N. A., Husain, F. M., Ahmed, F., Khan, R. A., Ahmad, I., Alsharaeh, E., & Aliev, G. (2016). Biogenic synthesis of zinc oxide nanostructures from *Nigella sativa* seed: Prospective role as food packaging material inhibiting broad-spectrum quorum sensing and biofilm. *Scientific Reports*, *6*(1), 1–16.

Anil, P., Nikhil, B., Manoj, G., & Prakash, N. B. (2012). Phytochemicals and biological activities of *Fagonia indica*. *International Research Journal of Pharmacy*, *3*, 56–59.

Aula, S., Lakkireddy, S., Swamy, A. V. N., Kapley, A., Jamil, K., Tata, N. R., & Hembram, K. (2014). Biological interactions in vitro of zinc oxide nanoparticles of different characteristics. *Materials Research Express*, *1* (3), 035041.

Azizi, S., Mohamad, R., Rahim, R. A., Moghaddam, A. B., Moniri, M., Ariff, A., & Namvab, F. (2016). ZnO-Ag core shell nanocomposite formed by green method using essential oil of wild ginger and their bactericidal and cytotoxic effects. *Applied Surface Science*, *384*, 517–524.

Babu, K. S., Reddy, A. R., Sujatha, C., Reddy, K. V., & Mallika, A. N. (2013). Synthesis and optical characterization of porous ZnO. *Journal of Advanced Ceramics*, *2*(3), 260–265.

Bagban, I. M., Roy, S. P., Chaudhary, A., Das, S. K., Gohil, K. J., & Bhandari, K. K. (2012). Hepatoprotective activity of the methanolic extract of *Fagonia indica* Burm in carbon tetra chloride induced hepatotoxicity in albino rats. *Asian Pacific Journal of Tropical Biomedicine*, *2* (3), S1457–S1460.

Barhoum, A., Van Assche, G., Rahier, H., Fleisch, M., Bals, S., Delplancked, M. P., & Bahnemann, D. (2017). Sol-gel hot injection synthesis of ZnO nanoparticles into a porous silica matrix and reaction mechanism. *Materials & Design*, *119*, 270–276.

Batool, R., Aziz, E., Iqbal, J., Salahuddin, H., Tan, B. K. H., Tabassum, S., & Mahmood, T. (2020). In vitro antioxidant and anti-cancer activities and phytochemical analysis of *Commelina benghalensis* L. root extracts. *Asian Pacific Journal of Tropical Biomedicine*, *10*(9), 417.

Bhuyan, T., Mishra, K., Khanuja, M., Prasad, R., & Varma, A. (2015). Biosynthesis of zinc oxide nanoparticles from *Azadirachta indica* for antibacterial and photocatalytic applications. *Materials Science in Semiconductor Processing*, *32*, 55–61.

Chaudhuri, S. K., & Malodia, L. (2017). Biosynthesis of zinc oxide nanoparticles using leaf extract of *Calotropis gigantea*: Characterization and its evaluation on tree seedling growth in nursery stage. *Applied Nanoscience*, *7*(8), 501–512.

Dejene, F., Ali, A., Swart, H., Botha, R., Roro, K., Coetsee, L., & Biggs, M. (2011). Optical properties of ZnO nanoparticles synthesized by varying the sodium hydroxide to zinc acetate molar ratios using a sol-gel process. *Open Physics*, *9*(5), 1321–1326.

Fatima, H., Khan, K., Zia, M., Ur-Rehman, T., Mirza, B., & Haq, I. U. (2015). Extraction optimization of medicinally important metabolites from *Datura innoxia* Mill. an in vitro biological and phytochemical investigation. *BMC Complementary and Alternative Medicine*, *15*(1), 1–18.

Fu, L., & Fu, Z. (2015). *Plectranthus amboinicus* leaf extract-assisted biosynthesis of ZnO nanoparticles and their photocatalytic activity. *Ceramics International*, *41*(2), 2492–2496.

Fuku, X., Matinise, N., Masikini, M., Kasinathan, K., & Maaza, M. (2018). An electrochemically active green synthesized polycrystalline NiO/MgO catalyst: Use in photo-catalytic applications. *Materials Research Bulletin*, *97*, 457–465.

Gondal, M. A., Drmosh, Q. A., Yamani, Z. H., & Saleh, T. A. (2009). Synthesis of ZnO2 nanoparticles by laser ablation in liquid and their annealing transformation into ZnO nanoparticles. *Applied Surface Science*, *256*(1), 298–304.

Haghniaz, R., Rabbani, A., Vajhadin, F., Khan, T., Kousar, R., Khan, A. R., & Wahid, F. (2021). Anti-bacterial and wound healing-promoting effects of zinc ferrite nanoparticles. *Journal of Nanobiotechnology*, *19*(1), 1–15.

Hameed, S., Ali Shah, S., Iqbal, J., Numan, M., Muhammad, W., Junaid, M., & Umer, F. (2020). Cannabis sativa-mediated synthesis of gold nanoparticles and their biomedical properties. *Bioinspired, Biomimetic and Nanobiomaterials*, *9*(2), 95–102.

Hameed, S., Iqbal, J., Ali, M., Khalil, A. T., Abbasi, B. A., Numan, M., & Shinwari, Z. K. (2019). Green synthesis of zinc nanoparticles through plant extracts: Establishing a novel era in cancer theranostics. *Materials Research Express*, *6*(10), 102005.

He, L., Liu, Y., Mustapha, A., & Lin, M. (2011). Antifungal activity of zinc oxide nanoparticles against *Botrytis cinerea* and *Penicillium expansum*. *Microbiological Research*, *166*(3), 207–215.

Iqbal, J., Abbasi, B. A., Ahmad, R., Batool, R., Mahmood, T., Ali, B., & Munir, A. (2019). Potential phytochemicals in the fight against skin cancer: Current landscape and future perspectives. *Biomedicine & Pharmacotherapy*, *109*, 1381–1393.

Iqbal, J., Abbasi, B. A., Ahmad, R., Mahmoodi, M., Munir, A., Zahra, S. A., & Capasso, R. (2020). Phytogenic synthesis of nickel oxide nanoparticles (NiO) using fresh leaves extract of *Rhamnus triquetra* (wall.) and investigation of its multiple in vitro biological potentials. *Biomedicines*, *8* (5), 117.

Iqbal, J., Abbasi, B. A., Ahmad, R., Shahbaz, A., Zahra, S. A., Kanwal, S., & Mahmood, T. (2020). Biogenic synthesis of green and cost effective iron nanoparticles and evaluation of their potential biomedical properties. *Journal of Molecular Structure*, *1199*, 126979.

Iqbal, J., Abbasi, B. A., Batool, R., Khalil, A. T., Hameed, S., Kanwal, S., & Mahmood, T. (2019). Biogenic synthesis of green and cost effective cobalt oxide nanoparticles using *Geranium wallichianum* leaves extract and evaluation of in vitro antioxidant, antimicrobial, cytotoxic and enzyme inhibition properties. *Materials Research Express*, *6*(11), 115407.

Iqbal, J., Abbasi, B. A., Mahmood, T., Hameed, S., Munir, A., & Kanwal, S. (2019). Green synthesis and characterizations of nickel oxide nanoparticles using leaf extract of *Rhamnus virgata* and their potential biological applications. *Applied Organometallic Chemistry*, *33*(8), e4950.

Iqbal, J., Abbasi, B. A., Mahmood, T., Kanwal, S., Ahmad, R., & Ashraf, M. (2019). Plant-extract mediated green approach for the synthesis of ZnONPs: Characterization and evaluation of cytotoxic, antimicrobial and antioxidant potentials. *Journal of Molecular Structure*, *1189*, 315–327.

Iqbal, J., Abbasi, B. A., Mahmood, T., Kanwal, S., Ali, B., Shah, S. A., & Khalil, A. T. (2017). Plant-derived anticancer agents: A green anticancer approach. *Asian Pacific Journal of Tropical Biomedicine*, *7*(12), 1129–1150.

Iqbal, J., Abbasi, B. A., Munir, A., Uddin, S., Kanwal, S., & Mahmood, T. (2020). Facile green synthesis approach for the production of chromium oxide nanoparticles and their different in vitro biological activities. *Microscopy Research and Technique*, *83*(6), 706–719.

Jafri, L., Saleem, S., Ullah, N., & Mirza, B. (2017). In vitro assessment of antioxidant potential and determination of polyphenolic compounds of *Hedera nepalensis* K. Koch. *Arabian Journal of Chemistry*, *10*, S3699–S3706.

Jangir, L. K., Kumari, Y., Kumar, A., Kumar, M., & Awasthi, K. (2017). Investigation of luminescence and structural properties of ZnO nanoparticles, synthesized with different precursors. *Materials Chemistry Frontiers*, *1*(7), 1413–1421.

Javed, R., Usman, M., Tabassum, S., & Zia, M. (2016). Effect of capping agents: Structural, optical and biological properties of ZnO nanoparticles. *Applied Surface Science*, *386*, 319–326.

Kadiyala, U., Turali-Emre, E. S., Bahng, J. H., Kotov, N. A., & VanEpps, J. S. (2018). Unexpected insights into antibacterial activity of zinc oxide nanoparticles against methicillin resistant *Staphylococcus aureus* (MRSA). *Nanoscale*, *10*(10), 4927–4939.

Kawakami, M., Hartanto, A. B., Nakata, Y., & Okada, T. (2003). Synthesis of ZnO nanorods by nanoparticle assisted pulsed-laser deposition. *Japanese Journal of Applied Physics*, *42*(1A), L33.

Khalil, A. T., Ovais, M., Iqbal, J., Ali, A., Ayaz, M., Abbas, M., … Devkota, H. P. (2021). Microbes-mediated synthesis strategies of metal nanoparticles and their potential role in cancer therapeutics. *Seminars in Cancer Biology*. https://doi.org/10.1016/j.semcancer.2021.06.006

Khalil, A. T., Ovais, M., Ullah, I., Ali, M., Shinwari, Z. K., Hassan, D., & Maaza, M. (2018). *Sageretia thea* (Osbeck.) modulated biosynthesis of NiO nanoparticles and their in vitro pharmacognostic, antioxidant and cytotoxic potential. *Artificial Cells, Nanomedicine, and Biotechnology*, *46*(4), 838–852.

Khalil, A. T., Ovais, M., Ullah, I., Ali, M., Shinwari, Z. K., Khamlich, S., & Maaza, M. (2017a). *Sageretia thea* (Osbeck.) mediated synthesis of zinc oxide nanoparticles and its biological applications. *Nanomedicine*, *12*(15), 1767–1789.

Khalil, A. T., Ovais, M., Ullah, I., Ali, M., Shinwari, Z. K., & Maaza, M. (2017b). Biosynthesis of iron oxide (Fe2O3) nanoparticles via aqueous extracts of *Sageretia thea* (Osbeck.) and their pharmacognostic properties. *Green Chemistry Letters and Reviews*, *10*(4), 186–201.

Khan, I., Ahmad, K., Khalil, A. T., Khan, J., Khan, Y. A., Saqib, M. S., & Ahmad, H. (2015). Evaluation of antileishmanial, antibacterial and brine shrimp cytotoxic potential of crude methanolic extract of Herb *Ocimum basilicum* (Lamiacea). *Journal of Traditional Chinese Medicine*, *35*(3), 316–322.

Kibasomba, P. M., Dhlamini, S., Maaza, M., Liu, C. P., Rashad, M. M., Rayan, D. A., & Mwakikunga, B. W. (2018). Strain and grain size of TiO2 nanoparticles from TEM, Raman spectroscopy and XRD: The revisiting of the Williamson-Hall plot method. *Results in Physics*, *9*, 628–635.

Lingaraju, K., Naika, H. R., Manjunath, K., Basavaraj, R. B., Nagabhushana, H., Nagaraju, G., & Suresh, D. (2016). Biogenic synthesis of zinc oxide nanoparticles using *Ruta graveolens* (L.) and their antibacterial and antioxidant activities. *Applied Nanoscience*, *6*(5), 703–710.

Lipovsky, A., Nitzan, Y., Gedanken, A., & Lubart, R. (2011). Antifungal activity of ZnO nanoparticles—The role of ROS mediated cell injury. *Nanotechnology*, *22*(10), 105101.

Liu, X., Wu, X., Cao, H., & Chang, R. P. H. (2004). Growth mechanism and properties of ZnO nanorods synthesized by plasma-enhanced chemical vapor deposition. *Journal of Applied Physics*, *95*(6), 3141–3147.

Lokesh, K., Kavitha, G., Manikandan, E., Mani, G. K., Kaviyarasu, K., Rayappan, J. B. B., … Maaza, M. (2016). Effective ammonia detection using n-ZnO/p-NiO heterostructured nanofibers. *IEEE Sensors Journal*, *16*(8), 2477–2483.

Malagoli, D. (2007). A full-length protocol to test hemolytic activity of palytoxin on human erythrocytes. *Invertebrate Survival Journal*, *4*(2), 92–94.

Matinise, N., Fuku, X. G., Kaviyarasu, K., Mayedwa, N., & Maaza, M. J. A. S. S. (2017). ZnO nanoparticles via *Moringa oleifera* green synthesis: Physical properties & mechanism of formation. *Applied Surface Science*, *406*, 339–347.

Mohamed, H. E. A., Afridi, S., Khalil, A. T., Zia, D., Iqbal, J., Ullah, I., & Maaza, M. (2019). Biosynthesis of silver nanoparticles from *Hyphaene thebaica* fruits and their in vitro pharmacognostic potential. *Materials Research Express*, *6*(10), 1050c9.

Nadhman, A., Khan, M. I., Nazir, S., Khan, M., Shahnaz, G., Raza, A., & Yasinzai, M. (2016). Annihilation of Leishmania by daylight responsive ZnO nanoparticles: A temporal relationship of reactive oxygen species-induced lipid and protein oxidation. *International Journal of Nanomedicine*, *11*, 2451.

Nadhman, A., Sirajuddin, M., Nazir, S., & Yasinzai, M. (2016). Photo-induced Leishmania DNA degradation by silver-doped zinc oxide nanoparticle: An in-vitro approach. *IET Nanobiotechnology*, *10*(3), 129–133.

Ouellette, M., Drummelsmith, J., Leprohon, P., El Fadili, K., Foucher, A., Vergnes, B., & Légaré, D. (2008). Drug resistance in Leishmania. In *Leishmania after the genome* (1st ed., pp. 159–176). Norfolk, England: Caister Academic Press.

Ovais, M., Nadhman, A., Khalil, A. T., Raza, A., Khuda, F., Sohail, M. F., & Shinwari, Z. K. (2017). Biosynthesized colloidal silver and gold nanoparticles as emerging leishmanicidal agents: An insight. *Nanomedicine*, *12*(24), 2807–2819.

Ovais, M., Raza, A., Naz, S., Islam, N. U., Khalil, A. T., Ali, S., & Shinwari, Z. K. (2017b). Current state and prospects of the phytosynthesized colloidal gold nanoparticles and their applications in cancer theranostics. *Applied Microbiology and Biotechnology*, *101*(9), 3551–3565.

Rahman, L., Shinwari, Z. K., Iqrar, I., Rahman, L., & Tanveer, F. (2017). An assessment on the role of endophytic microbes in the therapeutic potential of *Fagonia indica*. *Annals of Clinical Microbiology and Antimicrobials*, *16*(1), 1–12.

Raja, A., Ashokkumar, S., Marthandam, R. P., Jayachandiran, J., Khatiwada, C. P., Kaviyarasu, K., & Swaminathan, M. (2018). Eco-friendly preparation of zinc oxide nanoparticles using Tabernaemontana divaricata and its photocatalytic and antimicrobial activity. *Journal of Photochemistry and Photobiology B: Biology*, *181*, 53–58.

Rajakumar, G., Thiruvengadam, M., Mydhili, G., Gomathi, T., & Chung, I. M. (2018). Green approach for synthesis of zinc oxide nanoparticles from *Andrographis paniculata* leaf extract and evaluation of their antioxidant, anti-diabetic, and anti-inflammatory activities. *Bioprocess and Biosystems Engineering*, *41*(1), 21–30.

Rajan, R., Chandran, K., Harper, S. L., Yun, S. I., & Kalaichelvan, P. T. (2015). Plant extract synthesized silver nanoparticles: An ongoing source of novel biocompatible materials. *Industrial Crops and Products*, *70*, 356–373.

Saravanakkumar, D., Sivaranjani, S., Kaviyarasu, K., Ayeshamariam, A., Ravikumar, B., Pandiarajan, S., & Maaza, M. (2018). Synthesis and characterization of ZnO–CuO nanocomposites powder by modified perfume spray pyrolysis method and its antimicrobial investigation. *Journal of Semiconductors*, *39*(3), 033001.

Shah, A., Khalil, A. T., Ahmad, K., Iqbal, J., Shah, H., Shinwari, Z. K., & Maaza, M. (2021). Biogenic nanoparticles: Synthesis, mechanism, characterization and applications. In *Biogenic nanoparticles for cancer theranostics* (pp. 27–42). Amsterdam: Elsevier.

Singh, J., Kaur, N., Kaur, P., Kaur, S., Kaur, J., Kukkar, P., & Rawat, M. (2018). *Piper betle* leaves mediated synthesis of biogenic SnO2 nanoparticles for photocatalytic degradation of reactive yellow 186 dye under direct sunlight. *Environmental Nanotechnology, Monitoring and Management*, *10*, 331–338.

Thema, F. T., Manikandan, E., Dhlamini, M. S., & Maaza, M. (2015). Green synthesis of ZnO nanoparticles via *Agathosma betulina* natural extract. *Materials Letters*, *161*, 124–127.

Uddin, S., Safdar, L. B., Anwar, S., Iqbal, J., Laila, S., Abbasi, B. A., & Quraishi, U. M. (2021). Green synthesis of nickel oxide nanoparticles from *Berberis balochistanica* stem for investigating bioactivities. *Molecules*, *26*(6), 1548.

Uddin, S., Safdar, L. B., Iqbal, J., Yaseen, T., Laila, S., Anwar, S., & Quraishi, U. M. (2021). Green synthesis of nickel oxide nanoparticles using leaf extract of *Berberis balochistanica*: Characterization, and diverse biological applications. *Microscopy Research and Technique*. https://doi.org/10.1002/jemt.23756.

Ullah, I., Khalil, A. T., Ali, M., Iqbal, J., Ali, W., Alarifi, S., & Shinwari, Z. K. (2020). Green-synthesized silver nanoparticles induced apoptotic cell death in MCF-7 breast cancer cells by generating reactive oxygen species and activating caspase 3 and 9 enzyme activities. *Oxidative Medicine and Cellular Longevity*, *2020*, 1215395.

Ullah, I., Shinwari, Z. K., & Khalil, A. T. (2017). Investigation of the cytotoxic and antileishmanial effects of *Fagonia indica* L. extract and extract mediated silver nanoparticles (AgNPs). *Pakistan Journal of Botany*, *49*(4), 1561–1568.

Waheed, A., Barker, J., Barton, S. J., Owen, C. P., Ahmed, S., & Carew, M. A. (2012). A novel steroidal saponin glycoside from *Fagonia indica* induces cell-selective apoptosis or necrosis in cancer cells. *European Journal of Pharmaceutical Sciences*, *47*(2), 464–473.

Waters, B., Saxena, G., Wanggui, Y., Kau, D., Wrigley, S., Stokes, R., & Davies, J. (2002). Identifying protein kinase inhibitors using an assay based on inhibition of aerial hyphae formation in *Streptomyces*. *The Journal of Antibiotics*, *55*(4), 407–416.

Yadav, R. S., Mishra, P., & Pandey, A. C. (2008). Growth mechanism and optical property of ZnO nanoparticles synthesized by sonochemical method. *Ultrasonics Sonochemistry*, *15*(5), 863–868.

Yao, G., Sebisubi, F. M., Voo, L. Y. C., Ho, C. C., Tan, G. T., & Chang, L. C. (2011). Citrinin derivatives from the soil filamentous fungus Penicillium sp. H9318. *Journal of the Brazilian Chemical Society*, *22*(6), 1125–1129.

Zahra, S. A., Iqbal, J., Abbasi, B. A., Shahbaz, A., Kanwal, S., Shah, S. L., & Mahmood, T. (2021). Antimicrobial, cytotoxic, antioxidants, enzyme inhibition activities, and scanning electron microscopy of *Lactuca orientalis* (Boiss.) Boiss. seeds. *Microscopy Research and Technique*, *84*(6):1284–1295. https://doi.org/10.1002/jemt.23687.

Zahra, S. A., Iqbal, J., Abbasi, B. A., Yaseen, T., Hameed, A., Shahbaz, A., & Ahmad, P. (2021). Scanning electron microscopy of *Sophora alopecuroides* L. seeds and their cytotoxic, antimicrobial, antioxidant, and enzyme inhibition potentials. *Microscopy Research and Technique*, *84*(6):1–12. https://doi.org/10.1002/jemt.23740.

Zak, A. K., Razali, R., Abd Majid, W. H., & Darroudi, M. (2011). Synthesis and characterization of a narrow size distribution of zinc oxide nanoparticles. *International Journal of Nanomedicine*, *6*, 1399.

Zhang, X. H., Liu, Y. C., Wang, X. H., Chen, S. J., Wang, G. R., Zhang, J. Y., & Fan, X. W. (2005). Structural properties and photoluminescence of ZnO nanowalls prepared by two-step growth with oxygen-plasma-assisted molecular beam epitaxy. *Journal of Physics: Condensed Matter*, *17*(19), 3035.

How to cite this article: Hameed, S., Khalil, A. T., Ali, M., Iqbal, J., Rahman, L., Numan, M., Khamlich, S., Maaza, M., Ullah, I., Abbasi, B. A., Alasmari, F., & Shinwari, Z. K. (2021). Precursor effects on the physical, biological, and catalytic properties of *Fagonia indica* Burm.f. mediated zinc oxide nanoparticles. *Microscopy Research and Technique*, 1–17. https://doi.org/10.1002/jemt.23867